Isoelectronic Homologues and Isomers: Tropolone, 5-Azatropolone, 1-H-Azepine-4,5-dione, Saddle Points, and Ions†

Richard L. Redington

Department of Chemistry and Biochemistry, Texas Tech University, Lubbock, Texas 79409

Received: July 17, 2005; In Final Form: September 16, 2005

Computational studies of 12 64-electron homologues and isomers of tropolone in the S_0 electronic ground state are reported. Three minimum-energy structures, tropolone (Tp), 5-azatropolone (5Azt), and 5-H-5-azatropolonium ($5AztH^+$), have an internal H-bond and planar C_s geometry, and three, tropolonate (TpO^-), 5-azatropolonate ($5AzO^-$), and 1-H-azepine-4,5-dione (45Di), lack the H-bond and have twisted C_2 geometry. All 6 substances have an equal double-minimum potential energy surface and a saddle point with planar C_{2v} geometry. The energy for the gas-phase isomerization reaction 45Di → 5Azt is near +4 kJ mol^{-1} at the MP4(SDQ)/6-311++G(df,pd)//MP2/6-311++G(df,pd) (energy//geometry) theoretical level and around −20 kJ mol^{-1} at lower theoretical levels. The dipole moments computed for 45Di and 5Azt are 9.6 and 2.1 D, respectively, and this large difference contributes to MO-computed free energies of solvation that strongly favor—as experimentally observed—45Di over 5Azt in chloroform solvent. The MO-computed energy for the gas-phase protonation reaction 45Di + H^+ → $5AztH^+$ is −956.4 kJ mol^{-1}, leading to 926.8 kJ mol^{-1} as the estimated proton affinity for 45Di at 298 K and 1 atm. The intramolecular dynamical properties predicted for 5Azt and $5AztH^+$ parallel those observed for tropolone. They are therefore expected to exhibit spectral tunneling doublets. Once they are synthesized, they should contribute importantly to the understanding of multidimensional intramolecular H transfer and dynamical coupling processes.

1. Introduction

In 1945, Dewar reported that the chemistry of stipitatic acid could be explained by taking as its structure a carboxy-labeled derivative of the then unknown substance 2-hydroxy-2,4,6-cycloheptatriene-1-one. The latter was seen as of sufficient potential importance that Dewar proposed for it the name tropolone[1] (Tp, Figure 1A). Its chemistry, nonbenzenoid aromaticity, and apparent nonrigid character made tropolone and its derivatives subjects of immediate interest.[2,3] The experimental discovery of vibrational state-specific spectroscopic tunneling doublets in its ultraviolet (UV) vibronic[4−10] and infrared (IR) vibrational[11−15] spectra generated quantitative interest in its multidimensional tunneling properties.[16−18] Dynamical characteristics occurring in this 15-atom molecule are also expected to occur in more complex systems—perhaps even extending to the behaviors in enzyme−substrate complexes of H transfer enzymes.[19−21] The current broad general interest of tropolone and tropolonoids in chemistry and biochemistry can be seen by pairing the keyword "tropolone" with others such as "fungi", "bacteria", "cancer", or "cholchicine" in a web search. Many nitrogen heterocyclic compounds, including azepines, possess biological activity. While no article reporting the successful synthesis of 5-azatropolone (5Azt, Figure 1B) was located, its isomer 1-H-azepine-4,5-dione (45Di, Figure 2C) was reported by Bonacorso, Mack, and Effenberger.[22]

The purpose of the present research is to compare properties computed for the S_0 electronic ground states of the 12 64-electron isoelectronic tropolonoid configurations shown in Figures 1 and 2. The stable structures, 3 with internal H-bonds (Figure 1, C_s point group symmetry) and 3 without (Figure 2, twisted C_2 point group symmetry), each have equal double-minimum potential energy surfaces (PESs) and saddle point configurations with C_{2v} point group symmetry. Although only Tp, tropolonate ion ($C_7H_5O_2^-$, TpO^-), and 45Di are presently known experimentally, results computed for the set of 12 configurations are usefully compared with each other. Immediate goals of this computational research are as follows: (a) to examine prospects for the experimental preparation of 5Azt, $5AztH^+$, and $5AzO^-$; (b) to compare a few representative computed properties of the isoelectronic configurations sketched in Figures 1 and 2, structures so similar and yet so different; (c) to provide information useful to the analysis of vibrational state-specific spectroscopic tunneling structures observed for tropolone; and (d) to survey the nature of intramolecular dynamical behavior expected for 5Azt and $5AztH^+$. The computational methods are summarized in section 2. General comparative behavioral overviews are provided through the geometries (section 3) and charge distributions (section 4). Isomerization and protonation energetics are considered in sections 5−7. Vibrational spectra are briefly introduced in section 8, and a concluding discussion appears in section 9.

2. Computational Methods

Ab initio molecular orbital (MO) and density functional computations were performed on the molecules using the *Gaussian 98* codes.[23] Theoretical levels reaching the MP2/6-311++G(df,pd) level were used to compute fully optimized geometries at the minimum-energy and saddle point (SP) critical points—whereat energy values were recomputed at the MP4-(SDQ) level. Critical point properties were verified using "MP2/GEN" optimizations accompanied by computed (harmonic) vibrational spectra. The MP2/GEN computational level is favored in this work, because, without scaling, it yields an ordering and placement of the fundamental vibrations (in

† Part of the special issue "William Hase Festschrift".

10.1021/jp053928s CCC: $33.50
Published on Web 10/22/2005

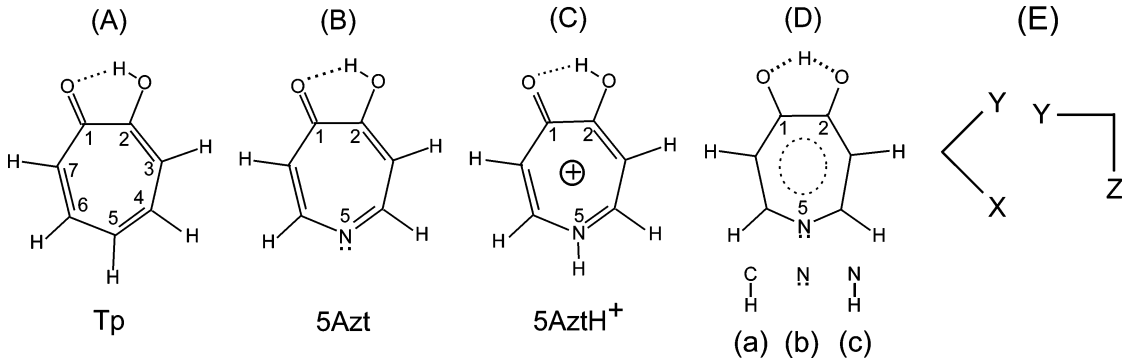

Figure 1. Minimum-energy structures for the isoelectronic molecules with C_s point group symmetry and an internal H-bond: (A) tropolone, Tp; (B) 5-azatropolone, 5Azt; (C) 5-H-5-azatropolonium, 5AztH$^+$. The three structures in (D) represent saddle point (SP) configurations with C_{2v} point group symmetry: (a) TpSP [C(5)H replaces N(5)]; (b) 5AztSP; and (c) 5AztH$^+$SP [N(5)H replaces N(5)]. The atom numbering for tropolone is used for all substances for convenience in Tables 1 and 2. (E) A diagram for use with Table 3 illustrating the in-plane axis orientations for the "standard configuration" of *Gaussian 98*: on left, approximate *XY* axis orientation for Tp, 5Azt, and 5AztH$^+$; on right, *YZ* axis orientation for the nine configurations having C_2 or C_{2v} point group symmetries. All coordinate origins occur at the center of nuclear charge.

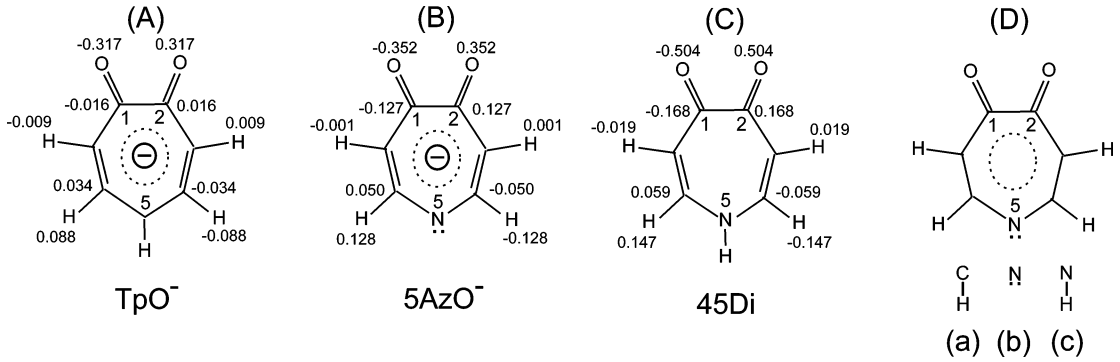

Figure 2. Minimum-energy structures for the isoelectronic molecules with C_2 point group symmetry: (A) tropolonate, TpO$^-$; (B) 5-azatropolonate, 5AzO$^-$; and (C) 1H-azepine-4,5-dione, 45Di. The three structures in (D) represent saddle point configurations with C_{2v} point group symmetry: (a) TpO$^-$SP [C(5)H replaces N(5)]; (b) 5AzO$^-$SP; and (c) 45DiSP [N(5)H replaces N(5)]. While the formal name for 45Di is used, in discussion the tropolone atom numbering is used. The numbers give out-of-plane atom displacements (Å) for the twisted structures—see footnote b of Table 2. Figure 1E shows the "standard" coordinate axis orientations.

harmonic approximation) that are in significantly closer agreement with the experimental IR spectra for Tp(OH) and Tp(OD) than either MP2-level computations using smaller basis sets or B3LYP/GEN level computations. Detailed comparisons of the MP2/GEN and B3LYP/GEN fundamentals with experimental data (which includes numerous assignable overtone, combination, and hot band transitions) appear in Redington et al.[12] In the present article including N atoms, the GEN basis is defined with 6-311G(df) functions for N and CO, 6-311G(pd) for the H in NH and in OHO, and 6-311G(d,p) for CH. The spectral computations utilized numerical second derivatives. MP2/GEN-level vibrational spectra computed for Tp and TpSP were previously used[12,16] to help analyze the experimental vibrational spectra and tautomerization properties of the Tp(OH) and Tp(OD) isomers. For comparison with the results of the described high-level computations, in the present work some of the geometry optimizations and spectral computations were also performed at lower theoretical levels, cf. MP2/6-31G** and B3LYP/6-31G**. Proton affinities at 25 °C and 1 atm were estimated using MP4(SDQ)/6-311++G(df,pd)//MP2/6-311++G(df,pd) (energy//geometry) electronic energies with data from MP2/GEN-computed harmonic frequencies.

3. Geometries

It is known through extensive comparisons with experimental data that geometrical parameters are among the most reliable of MO-computed results. Observed data are sparse for the present molecules, but bond distances and bond angles computed at the MP2/6-311++G(df,pd) level are nevertheless usefully intercompared, and Tables 1 and 2 provide an overview of structural differences arising within the isoelectronic systems. At this theoretical level, Tp, 5Azt, and 5AztH$^+$ are planar with C_s point group symmetry. TpO$^-$, 5AzO$^-$, and 45Di are twisted with C_2 point group symmetry and OCCO torsional angles of 11.87°, 13.34°, and 22.93°, respectively (the out-of-plane (*Z*) displacements for the atoms are presented in Figure 2A−C]. All six SP configurations are planar with C_{2v} point group symmetry.

The CH and NH bond distances are listed in lines 13−17 (3H−7H) of Table 1. The CH bond lengths within a molecule have a maximum spread of 0.004 Å (5Azt, 5AzO$^-$, and 5AzO$^-$ SP). Maximum spreads for specific CH bond lengths among all the molecules are 0.008 Å (4H, line 14) and 0.009 Å (6H, line 16). The NH bond lengths are 1.016 Å for 5AztH$^+$ (line 15) and 1.008 Å for 45Di. The spread of the average CO bond distances among molecules with H-bonds is 0.034 Å, versus 0.023 Å for molecules without H-bond. The average CO distance is 0.039 Å longer for the molecules with H-bonds than for those without H-bonds. For molecules with H-bonds, the average CO distance decreases by 0.004 or 0.005 Å upon SP formation; without H-bonds, the CO distances do not change. Line 1 shows that the O···O distance (the most variable of all heavy atom distances) decreases by 0.175 Å on average for molecules with the H-bond, versus 0.036 Å on average for molecules without an H-bond. The O···O distances in the SPs with O···H···O are 0.387, 0.408, and 0.378 Å shorter, and the

TABLE 1: Bond Distances (Å) Optimized at the MP2/6-311++G(df,pd) Level

		Tp	5Azt	5AztH$^+$	TpSP	5AztSP	5AztH$^+$SP	TpO$^-$	5AzO$^-$	45Di	TpO$^-$SP	5AzO$^-$SP	45DiSP	
		O···HO	O···HO	O···HO	OHO	OHO	OHO	O···O	O···O	O···O	O···O	O···O	O···O	
		CH	N	NH	CH	N	NH	CH	N	NH	CH	N	NH	
	ID[a]	C_s	C_s	C_s	C_{2v}	C_{2v}	C_{2v}	C_2[b]	C_2[b]	C_2[b]	C_{2v}	C_{2v}	C_{2v}	bond type
1	O···O	2.458	2.479	2.477	2.294	2.208	2.297	2.704	2.733	2.732	2.681	2.706	2.675	O···O
2	1O	1.251	1.245	1.228	1.285	1.278	1.255	1.245	1.240	1.222	1.245	1.240	1.222	CO
3	2O	1.326	1.321	1.289	1.285	1.278	1.255	1.245	1.240	1.222	1.245	1.240	1.222	CO
4	1OH	1.721	1.760	1.785	1.221	1.224	1.231							O···H
5	2OH	0.994	0.992	0.997	1.221	1.224	1.231							OH
6	12	1.472	1.474	1.504	1.472	1.475	1.510	1.520	1.518	1.535	1.524	1.521	1.542	CC
7	23	1.383	1.377	1.390	1.403	1.400	1.410	1.444	1.443	1.463	1.444	1.443	1.462	CC
8	34	1.403	1.412	1.384	1.389	1.393	1.370	1.388	1.386	1.356	1.388	1.386	1.356	CC
9[c]	45	1.383	1.316^N	1.336^N	1.396	1.335^N	1.357^N	1.397	1.342^N	1.368^N	1.397	1.342^N	1.367^N	CC or CN
10[c]	56	1.409	1.356^N	1.375^N	1.396	1.335^N	1.357^N	1.397	1.342^N	1.368^N	1.397	1.342^N	1.367^N	CC or CN
11	67	1.378	1.376	1.359	1.389	1.393	1.370	1.388	1.386	1.356	1.388	1.386	1.356	CC
12	71	1.434	1.433	1.443	1.403	1.400	1.410	1.444	1.443	1.463	1.444	1.443	1.462	CC
13	3H	1.086	1.086	1.085	1.086	1.086	1.085	1.089	1.089	1.085	1.089	1.089	1.085	CH
14	4H	1.086	1.090	1.085	1.087	1.089	1.085	1.091	1.093	1.085	1.091	1.093	1.085	CH
15[c]	5H	1.085		1.016^N	1.085		1.015^N	1.087		1.008^N	1.087		1.008^N	CH or NH
16	6H	1.087	1.088	1.084	1.087	1.089	1.085	1.091	1.093	1.085	1.091	1.093	1.085	CH
17	7H	1.087	1.086	1.085	1.086	1.086	1.085	1.089	1.089	1.085	1.089	1.089	1.085	CH

[a] Numbers refer to ring atoms 1−7 according to the tropolone scheme in Figure 1A. Bond types are shown in the right-most column. [b] Out-of-plane (*Z* coordinate) displacements for the atoms in molecules with C_2 symmetry (TpO$^-$, 5AzO$^-$, and 45Di) are shown in Figure 2. [c] Superscript N in lines 9, 10, and 15 indicates the bond incorporates an N atom.

TABLE 2: Bond Angles (deg) Optimized at the MP2/6-311++G(df,pd) Level

		Tp	5Azt	5AztH$^+$	TpSP	5AztSP	5AztH$^+$SP	TpO$^-$	5AzO$^-$	45Di	TpO$^-$SP	5AzO$^-$SP	45DiSP	
		O···HO	O···HO	O···HO	OHO	OHO	OHO	O···O	O···O	O···O	O···O	O···O	O···O	
		CH	N	NH	CH	N	NH	CH	N	NH	CH	N	NH	
	ID[a]	C_s	C_s	C_s	C_{2v}	C_{2v}	C_{2v}	C_2[b]	C_2[b]	C_2[b]	C_{2v}	C_{2v}	C_{2v}	bond type
1	OHO	127.65	126.26	123.30	140.03	139.70	137.91							OHO
2	O12	114.34	114.87	113.94	108.67	108.78	108.28	118.15	119.02	118.43	117.69	118.55	117.61	OCC
3	12O	110.66	111.28	111.50	108.67	108.78	108.28	118.15	119.02	118.43	117.69	118.55	117.61	CCO
4	2OH	100.66	101.29	103.77	91.32	91.37	92.77							COH
5	123	130.38	128.64	129.32	127.77	126.17	127.17	122.12	120.07	121.13	123.01	121.11	122.86	CCC
6	234	128.86	128.83	128.08	128.16	128.05	127.23	133.69	134.07	131.87	134.13	134.58	132.94	CCC
7[c]	345	129.12	132.71^N	129.48^N	129.79	133.25^N	129.68^N	130.12	133.99^N	129.63^N	130.28	134.18^N	129.92^N	CCC or CCN
8[c]	456	127.82	124.25^N	131.01^N	128.56	125.05^N	131.05^N	125.16	120.20^N	128.56^N	125.16	120.25^N	128.56^N	CCC or CNC
9[c]	567	130.18	133.32^N	129.16^N	129.79	133.25^N	129.68^N	130.12	133.99^N	129.63^N	130.28	134.18^N	129.92^N	CCC or NCC
10	671	130.33	130.56	130.18	128.16	128.05	127.23	133.69	134.07	131.87	134.13	134.58	132.94	CCC
11	712	122.34	121.70	122.77	127.77	126.17	127.17	122.12	120.07	121.13	123.01	121.11	122.86	CCC
12	23H	114.11	115.20	116.04	114.49	115.51	116.40	110.78	111.65	112.99	110.56	111.37	112.39	CCH
13	34H	115.04	114.01	117.20	114.91	114.23	117.54	114.44	113.61	117.87	114.32	113.47	117.64	CCH
14[c]	45H	116.20		114.66^N	115.72		114.08^N	117.42		115.7^N	117.42		115.72^N	CCH or CNH
15	76H	114.71	114.55	118.27	114.91	114.23	117.54	114.44	113.61	117.87	114.32	113.47	117.64	CCH
16	17H	112.68	113.52	114.11	114.49	115.51	116.40	110.78	111.65	112.99	110.56	111.37	112.39	CCH

[a] Numbers refer to ring atoms 1−7 according to the tropolone scheme in Figure 1A. Angle types are shown in the right-most column. [b] Out-of-plane (*Z* coordinates) displacements for the atoms in molecules with C_2 symmetry (TpO$^-$, 5AzO$^-$, and 45Di) are shown in Figure 2. [c] Superscript N in lines 7−9 and 14 indicates the angle incorporates an N atom.

CO distances are 0.040, 0.038, and 0.033 Å longer, than for systems lacking the H. The O···H distance decreases by about 0.5 Å upon formation of the SP (line 4).

Line 6 of Table 1 shows that the C(1)−C(2) distance of 5Azt, like that for Tp, is virtually unchanged by SP formation. Lines 7−12 show that there are very small changes of the CC and CN bond lengths upon SP formation for the systems without H-bond (where only the O···O and C(1)−C(2) distances show noteworthy changes). Other than CN versus CC bonds, the geometries of TpO$^-$ and 5AzO$^-$ are similar. The C−C bond distances in 45Di are longer, and the C=C bond distances are shorter, than those in the anions. The CN bond distance in 45Di is 0.032 Å longer than the average value in 5Azt. 45Di is the most twisted molecule (Figure 2C). Tables 1 and 2 show a clear dispersion of bond distance and bond angle values among the 12 local PES regions. These computed dispersions are expected to reflect prospective experimental dispersions for the geometries and for other molecular properties.

The planar geometries computed for Tp, 5Azt, and 5AztH$^+$ in the S_0 electronic state suggest that interactions due to H-bonding and to the π resonance eclipse the opposing drives toward nonplanar structures. The latter drives include the relaxation of parallel CO bond energy by OCCO torsion and the relaxation of ring strain by kinking. The CC distances in lines 8 and 11 (nominal C(3)−C(4) single and C(6)=C(7) double bonds) reflect the presence of appreciable π resonance interactions in the molecules with an H-bond. These MO-computed bond distances differ by about 0.03 Å, far less that

TABLE 3: Comparative Nonzero Electric Dipole (*D*) and Quadrupole (*D*·Å) Moment Components Listed with MP4(SDQ)/6-311++G(df,pd) Output

		Tp	5Azt	5AztH$^+$	TpSP	5AztSP	5AztH$^+$SP	TpO$^-$	5AzO$^-$	45Di	TpO$^-$SP	5AzO$^-$SP	45DiSP
		O···HO	O···HO	O···HO	OHO	OHO	OHO	O···O	O···O	O···O	O···O	O···O	O···O
		CH	N	NH	CH	N	NH	CH	N	NH	CH	N	CH
	param.[a]	C_s	C_s	C_s	C_{2v}	C_{2v}	C_{2v}	C_2	C_2	C_2	C_{2v}	C_{2v}	C_{2v}
1	charge	0	0	+1	0	0	+1	−1	−1	0	−1	−1	0
2	dipole	4.718	2.104	7.388	5.175	2.329	7.739	6.727	4.163	9.612	6.812	4.238	9.769
3	*X*[b]	3.676	2.032	5.761									
4	*Y*	−2.957	−0.547	−4.626									
5	*Z*				5.175	2.329	7.739	6.727	4.163	9.612	6.812	4.238	9.769
6	*XX*	−53.91	−55.87	−35.13	−55.85	−53.69	−51.76	−59.70	−57.30	−55.19	−59.06	−56.56	−54.00
7	*YY*	−49.58	−53.28	−30.41	−49.54	−47.43	−38.02	−63.59	−61.13	−49.55	−64.09	−61.69	−50.44
8	*ZZ*	−55.90	−53.75	−51.83	−54.71	−62.48	−28.89	−79.45	−86.08	−52.40	−79.71	−86.48	−52.77
9	*XY*	1.60	6.50	−5.77				2.38	2.66	−3.12			
10	Q_{ave}	−53.13	−54.30	−39.12	−53.37	−54.53	−39.56	−67.58	−68.17	−52.38	−67.62	−68.24	−52.40
11	*R*	0.119	0.048	0.548	0.118	0.276	0.578	0.293	0.422	0.108	0.305	0.438	0.068

[a] $Q_{ave} = (XX + YY + ZZ)/3$. For columns 3−5, *Z* is the out-of-plane axis. For columns 6−14, *Z* is the C_2 rotational axis. $R = (Q_{max} - Q_{min})/Q_{ave}$, where Q_{max} is the largest and Q_{min} is the smallest of the *XX*, *YY*, and *ZZ* values. [b] The coordinate origins are at the nuclear center of charge within the heptacyclic ring. The origins and the axis orientations are available from the C(1) and C(2) atom positions: Tp(−1.139, 0.142, 0; 0, 1.077, 0). TpSP(0, 0.736, −0.816; 0, −0.736, −0.816). 45Di(0.168, 0.749, −0.972; −0.168, −0.749, −0.972). 45DiSP(0, 0.771, −0.978; 0, −0.771, −0.978). The coordinate origins and axis orientations within each triad (e.g., for Tp, 5Azt, and 5AztH$^+$) are quite similar.

the 0.20 Å difference obtained between the tabulated[24] values used for "standard" CC single and double bonds [*R*(C−C) − *R*(C=C) = 1.54 − 1.34 = 0.20 Å]. Comparative CC bond distances suggest that π interactions in 5Azt are weaker than those in Tp. Distances computed for nominal C=O and C=C bonds, respectively, of 45Di are near the standard values of 1.23 and 1.34 Å. The nominal C−C distances [C(2)−C(3) and C(1)−C(2)] are 1.463 and 1.535 Å, respectively, versus the 1.54 Å standard. The MO-computed CN distance in 45Di is 1.368 Å, a value 0.015 Å longer than that observed for pyridine. Optimization at the MP2/6-311G(df,pd) level yields CN distances of 1.367 and 1.339 Å for pyrrole and pyridine, respectively, with ∠CNC angles of 110.23° and 116.59°. The CN bond distance of 45Di is close to that in pyrrole, while the average of the two CN distances in 5Azt is 0.003 Å less than the computed CN distance in pyridine. The lack of an internal H-bond and the weakness of the computed π resonance interactions allow nonplanar geometries to be induced for TpO$^-$, 5AzO$^-$, and 45Di by the drives to relax ring strain and cis C=O groups. However, the barrier maxima for their C_{2v} SPs are only 1−2 kJ mol^{-1} (vida infra). It is noted that minimum-energy geometries for 45Di computed at the B3LYP/6-31G** and MP2/6-31G** levels are not twisted, but planar with C_{2v} symmetry. Glyoxal and oxalyl fluoride both show primary trans and secondary cis energy minima at the MP4(SDQ)/6-311G(df,pd) level.

Geometrical parameters computed for the six stable isoelectronic configurations are expected to agree well with experimental measurements, but there are few opportunities for comparison. Tanaka et al.[25] used microwave spectroscopy to evaluate accurate rotational constants for Tp(OH). The present MO-computed values, $A = 2.7767$, $B = 1.6592$, and $C = 1.0386$ GHz, reflect the geometry at a PES minimum and are +1.2% higher, −0.04% lower, and +0.41% higher, respectively, than the experimental values. The latter reflect the equilibrium geometry for the nonrigid Tp(OH) molecule at ambient temperature. In the crystal, the tropolone molecules are dimerized through intermolecular H-bonds,[26] and the monomer geometry in this state differs somewhat from that in the gas phase. The average difference between the calculated (monomer) and crystalline (dimeric) bond distances is 0.009 Å when the C(4)-C(5), C(4)H, and OH distances are excluded. For these, the MO-computed distances are longer by 0.042, 0.046, and 0.05 Å, respectively. In the crystal, the monomer is slightly nonplanar with the seven-membered ring bent into a weak boat configuration having 2.4° and 1.2° bending angles. The average difference between the computed monomer and the crystalline ∠CCC bond angles is 0.9°. This value is reduced to 0.5° when angles defined using the C(1)C(2) axis are excluded. For other angles involving the five-membered ring, cf., angles O12, 12O, and 2OH (lines 2−4 in Table 2), the MO-computed monomer angles are 1.1°, 4.0°, and 6.3° smaller than observed in the crystal. The average difference of the calculated CCH angles in Table 2 and the crystallographic angles is 1.0°.

4. Electric Dipole and Quadrupole Moments

The relative charge distributions arising in the twelve isoelectronic systems affect not only the solvation free energy values discussed in the following section, but also many other inter- and intramolecular properties. Table 3 samples the diversiform charge patterns computed for the molecules as represented by the electric dipole and quadrupole moments accompanying the MP4(SDQ)6-311++G(df,pd) level outputs. Dipole components for the ions, and for all quadrupole components, depend on the origin of the coordinate system—here, the center of nuclear charge computed for the "standard" coordinate system by the Gaussian[23] code. For each triad of molecules in Table 3 (cf., Tp, 5Azt, 5AztH$^+$, footnote b), the origins lie in a close cluster within the heptacyclic ring near the C(1)−C(2) bond. *Z* is the out-of-plane coordinate for Tp, 5Azt, and 5AztH$^+$. For these molecules, the *XY* system must be rotated counterclockwise by roughly 45° about *Z* to bring *Y* into parallel with the fictive C_2 axis (see Figure 1E, left side). For the molecules with C_2 and C_{2v} geometries, *Z* is the axis of twofold rotational symmetry and *X* is the out-of-plane coordinate. For all twelve configurations, the dipole vector is directed toward the C(5) or N(5) region. The dipole moment magnitudes listed in line 2 of Table 3 range between 2.10 D for 5Azt and 9.77 D for 45DiSP.

The dipole moment relationship $\mu_{5Azt} = 2.10 < \mu_{Tp} = 4.72 \ll \mu_{45Di} = 9.61$ D is independent of the coordinate origins and is anticipated from elementary arguments. The O···HO and N group dipoles of 5Azt are oppositely directed to subtract and predict $\mu_{5Azt} < \mu_{Tp}$ (which lacks the N:), while the similarly directed CO···CO and NH group dipoles in 45Di add to predict $\mu_{45Di} > \mu_{Tp}$. In 5Azt, there is a roughly 30° rotation of the μ_{5Azt}

TABLE 4: Computed Energies E(5Azt) − E(45Di) (kJ mol^{-1}) for the Gas-Phase Isomerization Reaction 45Di → 5Azt

	6-31G**	6-31++G**	GEN[a]	GEN++	6-311G(df,pd)[b]	6-311++G(df,pd)[c]
B3LYP	−23.16	−19.08	−15.25	−14.46	−14.56	−14.08
MP2	−19.10	−15.89	−22.69	−21.70	−20.17	−19.16
MP3	−9.77	−7.66	−11.26	−11.29	−7.93	−8.00
MP4(SD)	1.02	3.26	0.16	0.25	3.76	3.79
MP4(SDQ)	0.77	3.79	−0.47	0.47	3.04	3.91[d]

[a] The GEN basis is defined in section 2. [b] The individual molecule energies (in H) in column 6 are E(5Azt) − E(45Di): (−436.94350778) − (−436.93796251); (−435.88717726) − (−435.87949450); (−435.89915405) − (−435.89613211); (−435.89099667) − (−435.89243018); (−435.91198271) − (−435.91313986). [c] The individual molecule energies (in H) in column 7 are E(5Azt) − E(45Di): (−436.95486283) − (−436.94950145); (−435.90470900) − (−435.89741220); (−435.91446992) − (−435.91142401); (−435.90623787) − (−435.90768303); (−435.92747565) − (−435.92896306). [d] The correction for the thermal contribution to the free energy at 25 °C and 1 atm yields the estimate $\Delta G^{\circ}_{\mathrm{isom,298K}} = 3.91 + 0.84 = 4.8$ kJ mol^{-1}. See text.

TABLE 5: Computed Free Energies of Solvation, $\Delta G^{o}_{\mathrm{solv,298K}}$ (kJ mol^{-1}), for Isoelectronic Substances Dissolved in $HCCl_3$

theoretical level[a]	45Di	45DiSP	5Azt	Tp	5AztH$^+$	TpO$^-$	5AzO$^-$
B3LYP/GEN	−31.5	−30.7	−11.3	−8.3	−165.2		
B3LYP/6-311G(df,pd)	−32.1	−32.3	−8.5	−7.6	−165.3		
MP4(SDQ)/GEN	−36.3	−37.0	−11.8	−11.8	−169.8	−168.0	−175.1
MP4(SDQ)/6-311G(df,pd)	−36.5	−37.5	−11.4	−11.4	−169.8		
MP4(SDQ)/6-311++G(df,pd)	−37.9	−40.17	−13.3	−13.9	−171.2	−179.3	−170.1

[a] Self-consistent reaction field (SCRF) method with the polarized continuum (overlapping spheres) model.[29]

dipole vector away from the fictive C_2 axis (cf., lines 3 and 4 of Table 3). The dipole moments are sensitive to the level of MO computation, and the values listed in Table 3 for Tp, 5Azt, 5AztH$^+$, and 45Di, for example, are 6.8%, 9.5%, 2.1%, and 2.5% larger, respectively, than values computed without using the ++ diffuse functions.

The nonzero quadrupole moment components are listed in lines 6−9 of Table 3. These show the out-of-plane components (*ZZ* for Tp, 5Azt, and 5AztH$^+$ and *XX* for the other nine substances) are of similar magnitude. The spread mainly reflects the values computed for the oppositely charged ions (cf., −51.76 for 5AztH$^+$SP and −59.70 for TpO$^-$). Average values for the three diagonal quadrupole components, Q_{ave} in line 10, and the quantities $R = (Q_{\mathrm{max}} - Q_{\mathrm{min}})/Q_{\mathrm{ave}}$ listed in line 11, reflect the charge distributions. R is zero for a spherical charge distribution and, except for 5AztSP, R values computed for the neutral species are <0.12. Except for 5Azt and 5AztSP, R values computed for the stable and SP configurations of each substance are similar. For 5Azt, $R = 0.048$, and for 5AztSP, $R = 0.276$ to indicate that a significant charge redistribution accompanies the transformation of 5Azt to 5AztSP. Not surprisingly, some Mulliken charges computed for the twelve isoelectronic systems appear to be inappropriate. They are not tabulated here, but the most suspect is for C(6). For this atom, the average charge of −0.617 falls between the extremes of −0.365 for TpSP and −0.779 for 5Azt. The charge distributions for Tp, TpO$^-$, and $C_7H_7O_2^+$ were considered by Mó et al.[27] using computed charge densities, their Laplacians, and atoms-in-molecules theory.[28]

The high polarity and geometrical shape computed for 45Di are suggestive of solid-state packing producing a relatively high melting point, and Bonacorso et al.[22] report that the observed value is higher than 280 °C. State-specific dipole moment values for gaseous Tp were determined by Tanaka et al.[25] from Stark effect measurements on two low-J rotational transitions for each of the 0^+ and 0^- tunneling forms. The values are 3.428 and 3.438 D, significantly less than the computed value of 4.72 D listed in Table 3. The large MO-computed dipole moment for 45Di (9.61 D) is placed in perspective by a compilation[24] of about 800 experimental values for gaseous molecules. The 4 or 5 D range is seen to be on the high side for ordinary organic molecules. An exceptionally large value is 5.78 ± 0.11 D (2-pyridinecarbonitrile) with a more typical value being 3.66 ± 0.11 D (3-pyridinecarbonitrile). Only the dipole moments for some diatomic alkali halides exceed the MO-computed 9.61 D estimate for 45Di.

5. The Energy of Isomerization and Relative $\Delta G_{\mathrm{solvation}}$ Values for 45Di and 5Azt

Bonacorso et al.[22] found no evidence for 5Azt in ^{1}H and ^{13}C NMR spectra of 45Di dissolved in $DCCl_3$, and the MO computations presented in this section agree with this observation. Theoretical energy values for the gas-phase isomerization reaction 45Di → 5Azt are presented in Table 4. The correlation energy approximation is important to the results, and only at the MP4(SD) and MP4(SDQ) levels does the energy of 45Di fall below that of 5Azt—by up to about 4 kJ mol^{-1}. For reference, the individual molecular energies (in hartrees) for columns 6 and 7 are included as footnotes to Table 4. As is customary for MPn computations, the MP2, MP3, MP4(SD), and MP4(SDQ) energy values oscillate. While the molecular energies for these 64-electron systems are not converged in these computations, the present objective is to estimate energy differences. The entries of Table 4 and subsequent tables indicate better convergence for the various differences than occurs for the molecular energies themselves. *Unscaled* harmonic MP2/GEN-level frequencies (section 2) produce the zero-point (ZP) energy difference EZP(5Azt) − EZP(45Di) = −0.23 kJ mol^{-1}. The thermal contribution of the translation, rotation, and vibration energies to the standard free energy for the gas-phase isomerization reaction is computed as 187.248 − 186.405 = 0.84 kJ mol^{-1}. Using this MP2/GEN-computed thermal correction value with the MP4(SDQ)/6-311++G(df,pd) electronic energy difference from Table 4 yields the estimate $\Delta G^{\circ}_{\mathrm{isom,298K}} = 3.91 + 0.84 = 4.8$ kJ mol^{-1} for the standard free energy of the gas-phase isomerization reaction 45Di → 5Azt.

The disparity between the dipole moment values $\mu_{45\mathrm{Di}} = 9.61$ and $\mu_{5\mathrm{Azt}} = 2.10$ D leads to a large difference of $DCCl_3$ solvation interactions. With the solvation interaction included, the free energy difference favoring 45Di over 5Azt increases to about 25 kJ mol^{-1} at 298 K and 1 atm. The MO-computed estimates for the free energy of solvation are listed in columns 2 and 4 of Table 5. They were determined using the self-consistent reaction field (SCRF) method with the polarized continuum (overlapping spheres) model of Tomasi and co-workers.[29] The computed

TABLE 6: Computed Energies (kJ mol^{-1}) for the Protonation Reaction 45Di + H$^+$ → 5AztH$^+$ and for Two Isomerization Reactions of 5AztH$^+$

	protonation reaction[a]			isomerization reation[b]					
	E(5AztH$^+$) − E(45Di)			E(NC$_6$H$_4$O$_2$H$_2^+$) − E(5AztH$^+$)			E($^+$H$_2$NC$_6$H$_4$O$_2$) − E(5AztH$^+$)		
	6-31++G**	GEN++	6-311++G(df,pd)	6-31G**	GEN	6-311G(df,pd)	6-31G**	GEN	6-311G(df,pd)
B3LYP	−964.7	−962.7	−962.5	58.8	61.7	62.0	234.7	233.7	233.3
MP2	−950.5	−961.1	−957.0	51.2	50.1	51.1	207.9	217.9	214.0
MP3	−961.2	−970.3	−966.1	49.5	48.1	49.9	189.1	197.1	192.8
MP4(SD)	−952.0	−960.6	−956.6	56.2	54.8	57.0	173.2	181.1	177.0
MP4(SDQ)	−951.7	−960.4	−956.4[c]	65.6	64.4	66.4	179.9	187.0	183.1

[a] The following sets list the protonation energies computed without including the ++ diffuse functions. 6-31G** column: −969.0, −960.9, −975.5, −977.6, −978.7 kJ mol^{-1}. GEN column: −961.0, −955.5, −971.8, −973.8, −974.3 kJ mol^{-1}. 6-311G(df,pd) column: −961.3, −953.7, −970.7, −973.2, −973.5 kJ mol^{-1}. [b] Note these basis sets exclude the ++ diffuse functions. The optimized geometry of NC$_6$H$_4$O$_2$H$_2^+$ has planar C_s point group symmetry, and $^+$H$_2$NC$_6$H$_4$O$_2$ is constrained to have C_{2v} point group symmetry. The MP2/GEN vibrational spectrum was not computed. At the B3LYP/6-311G(df,pd) level, there are two imaginary frequencies at the optimized geometry. [c] For this reaction energy, the estimated standard enthalpy is $\Delta H°_{\text{react,298 K}}$ = −926.8 kJ/mol^{-1} yielding the proton affinity PA(45Di) = 926.8 kJ/mol^{-1}. See text.

results are thermodynamically consistent with the failure of Bonacorso et al.[22] to observe the rise of 5Azt transitions in NMR spectroscopy experiments performed on 45Di dissolved in $DCCl_3$. Results of the MP4 level computations in columns 2 and 3 of Table 5 suggest the possibility that 45Di may take planar rather than twisted configurations in highly polar solvents. The SCRF-computed free energies of solvation for Tp, 5AztH$^+$, TpO$^-$, and 5AzO$^-$ dissolved in chloroform are included for reference in Table 5.

6. Protonation of 5Azt, 45Di, TpO$^-$, and 5AzO$^-$

The protonation reactions of gaseous and solvated 5Azt and 45Di are important considerations with respect to future experiments. Figures 1B and 2C show that protonation of the N atom of 5Azt, or of an O atom of 45Di, yields (HN)C$_6$H$_4$(OHO)$^+$. This ion is labeled 5AztH$^+$ and is informally called 5-H-5-azatropolonium (Figure 1C). Table 6 presents electronic energy values computed for the gas-phase protonation reaction 45Di + H$^+$ → 5AztH$^+$. They are relatively insensitive to the level of MO computation, and at the MP4(SDQ)/6-311++G(df,pd)//MP2/6-311++G(df,pd) level, the value for the reaction energy is −956.4 kJ mol^{-1}. The energies for two higher-energy isomer configurations were also computed, and these values relative to that of 5AztH$^+$ are included in Table 6. For the highest-level computation, the NC$_6$H$_4$O$_2$H$_2^+$ isomer, with HO•••HO moiety and C_s point group symmetry, is +66.4 kJ mol^{-1} above 5AztH$^+$. The $^+$H$_2$NC$_6$H$_4$O$_2$ isomer, with $^+$H$_2$N moiety and its geometry constrained to nonplanar C_{2v} symmetry, is +183.1 kJ mol^{-1} above 5AztH$^+$. At the B3LYP/6-311G(df,pd) level, the C_{2v} configuration corresponds to a second-degree saddle point with two imaginary vibrational frequencies rather than to an energy minimum.

Unscaled MP2/GEN-computed fundamentals yield 307.53 − 270.90 = 36.6 kJ mol^{-1} as the ZP energy difference EZP(5AztH$^+$) − EZP(45Di) of the protonation reaction. At this level, the thermal contribution to the enthalpy of the reaction is 328.88 − 293.06 − 5RT/2 = 29.61 kJ mol^{-1}. In combination with the −956.4 kJ mol^{-1} energy value, this yields −926.8 kJ mol^{-1} as the estimated standard reaction enthalpy. The corresponding proton affinity for 45Di is then PA(45Di) = 926.8 kJ mol^{-1} at 298 K and 1 atm. The value for 5Azt, PA(5Azt) = 921.5 kJ mol^{-1}, is obtained similarly: −(−952.5 + 328.88 − 291.72 − 6.20) = +921.5 kJ mol^{-1}. The enthalpy for protonation of the N in 5Azt and for an O in 45Di are thus closely matched. These computed PA values compare well with values observed for related molecules.[30] The value for PA(45Di) is similar to the value observed for pyridine—PA(pyridine) = 930.0 kJ mol^{-1}—and located in the midst of the observed values PA(NH$_3$) = 853.6, PA[(CH$_3$)NH$_2$] = 899.0, PA[(CH$_3$)$_2$NH] = 929.5, and PA[(CH$_3$)$_3$N] = 938.9 kJ mol^{-1}. PA(5Azt) = 921.5 kJ mol^{-1} is higher than the values generally observed for protonation of keto groups,[30] e.g., PA(*p*-benzoquinone) = 799.1, PA(*c*-hexane-1,2-dione) = 849.6, PA(*c*-hexane-1,3-dione) = 881.2, but it is in line with PA(2,6-dimethyl-4-pyrone) = 941.5 kJ mol^{-1}, for which keto and ether O atoms are opposite across the six-membered ring. For tropolone, the experimentally observed value PA(Tp) = 894.1 kJ mol^{-1} was reported by Mó et al.[27] The large proton affinity calculated for gaseous 45Di suggests forming 5AztH$^+$ via gas-phase or solution-phase protonation reactions of 45Di with suitable H$^+$ donors.

TABLE 7: Computed Gas-Phase Protonation Energies (kJ mol^{-1}) for TpO$^-$ + H$^+$ → Tp and 5AzO$^-$ + H$^+$ → 5Azt

	E(Tp) − E(TpO$^-$)		E(5Azt) − E(5AzO$^-$)
	6-31++G**	6-311++G(df,pd)	6-311++G(df,pd)
B3LYP	−1451.5	−1451.2	−1406.3
MP2	−1454.6	−1462.3	−1413.7
MP3	−1479.2	−1484.2	−1434.9
MP4(SD)	−1474.2	−1478.1	−1428.1
MP4(SDQ)	−1465.3	−1470.1[a]	−1421.2[a]

[a] Correction for the thermal contribution to the enthalpy at 25 °C and 1 atm yields the estimated standard gas-phase enthalpies of reaction $\Delta H°_{\text{react,298K}}$(TpO$^-$) = −1439 kJ/mol^{-1} and $\Delta H°_{\text{react,298K}}$(5AzO$^-$) = −1391 kJ/mol^{-1} for these energy points. See text.

MO-computed energies for the gas-phase protonation−neutralization reactions TpO$^-$ + H$^+$ → Tp and 5AzO$^-$ + H$^+$ → 5Azt are listed in Table 7. MP2/GEN-computed thermal contributions to the standard enthalpies are 322.00 − (282 + 3) − 6.20 = 31 and 291.72 − (253 + 3) − 6.20 = 30 kJ mol^{-1}, respectively, where 3 kJ mol^{-1} is added to the enthalpy thermal contribution for each reaction. This is because MP2/GEN-computed vibrational spectra for only the C_{2v} anion configurations were performed. These were thereby discovered to be SPs, and vibrational spectra were not computed for the lower-energy C_2 configurations. The difference of the thermal enthalpy contributions computed for 45Di and 45DiSP is 3 kJ mol^{-1}, and this value was used as an estimate for correcting the ion enthalpies. The approximate standard reaction enthalpies are then −1439 and −1391 kJ mol^{-1} for the gas-phase reactions at 25 °C and 1 atm. Reversing the signs yields estimated proton affinities for gaseous TpO$^-$ and 5AzO$^-$ that are of the same magnitude observed[30] for the neutrals Na$_2$O and Cs$_2$O, i.e., PA(Na$_2$O) = 1375.9 and PA(Cs$_2$O) = 1442.9 kJ mol^{-1}. MO-

TABLE 8: Computed Saddle Point Barriers (kJ mol^{-1}) for Tropolonoids with Internal H-Bonds

	E(TpSP) − E(Tp)			E(5AztSP) − E(5Azt)			E(5AztH$^+$SP) − E(5AztH$^+$)		
	6-31++G**	GEN++	6-311++G(df,pd)	6-31++G**	GEN++	6-311++G(df,pd)	6-31++G**	GEN++	6-311G++(df,pd)
B3LYP	21.29	22.67	22.69	21.90	22.98	23.06	24.26	24.67	24.67
MP2	23.48	15.57	15.67	26.15	17.71	17.91	25.24	15.80	15.90
MP3	39.84	30.26	30.39	42.05	32.13	32.28	40.23	29.01	29.11
MP4(SD)	42.47	33.20	33.31	44.46	34.91	35.02	41.62	30.93	30.98
MP4(SDQ)	38.06	29.58	29.70	39.35	30.71	30.80	36.42	26.99	27.00

TABLE 9: Computed Saddle Point Barriers (kJ mol^{-1}) for O···O Tropolonoids

	E(TpO$^-$SP) − E(TpO$^-$)		E(5AzO$^-$SP) − E(5AzO$^-$)		E(45DiSP) − E(45Di)	
	6-31++G**	6-311++G(df,pd)	6-31++G**	6-311++G(df,pd)	6-31++G**	6-311G++(df,pd)
B3LYP	0.00	0.00	0.00	0.00	0.00	0.00
MP2	0.00	1.34	0.00	1.35	1.97	2.00
MP3	0.00	0.93	0.00	0.89	1.89	1.70
MP4(SD)	0.00	0.96	0.00	0.96	2.00	1.86
MP4(SDQ)	0.00	0.82	0.00	0.88	2.03	1.85

computed free energy of solvation estimates for the anions are included in Table 5.

7. PES Saddle Point Energy Maxima

The SP barrier energies E(SP) − E(min) computed for Tp, 5Azt, and 5AztH$^+$ are listed in Table 8. At the highest utilized theoretical level, the SP barrier maxima computed for 5Azt and 5AztH$^+$ are 30.80 and 27.00 kJ mol^{-1}, respectively—values 1.10 kJ mol^{-1} (3.7%) higher and 2.70 kJ mol^{-1} (9.1%) lower than the 29.70 kJ mol^{-1} barrier computed for Tp. The similar molecular geometries, SP barriers, and vibrational spectra computed for Tp, 5Azt, 5AztH$^+$ and their SP configurations suggest they possess similar skeletal contortion and tautomerization behaviors. However, the limited PES samplings are only first indicators of the vibrational state-dependent *effective* PESs, because the latter incorporate geometry-dependent vibrational energies for each state under consideration. The MO-computed SP barrier maxima computed for TpO$^-$, 5AzO$^-$, and 45Di are listed in Table 9. These particular results predict that the skeletal twisting is hindered by barriers of only 1 or 2 kJ mol^{-1} (e.g., 80−170 cm^{-1}), a result that is realistically summarized by simply stating that quite high level MO computations can only predict that a low barrier (energy difference) separates the two conformers. When spectroscopic data are obtained to definitively settle the relative energetics question by experiment, it is likely that work by Laane and his group[31] will be of interest in the analyses. They have addressed the development of molecular Hamiltonians and the analysis of contortion spectra for molecules showing puckering or pseudorotation motions.

8. Vibrational Spectra

Details of the comparative MP2/GEN-computed fundamental vibrational spectra and normal coordinates obtained for the twelve isoelectronic structures will be presented in a separate article. Energy states for the six nonrigid molecules are classified according to the G_4 molecular symmetry group,[32] which is isomorphic to the C_{2v} point group. Thus, the a′ and a″ vibrational fundamentals computed in harmonic approximation for the planar C_s molecules, for example, are sorted into the in-plane a_1 and b_2 and the out-of-plane a_2 and b_1 irreducible representations of G_4. The fundamental frequencies and normal coordinates are useful progenitors for preparing a preliminary mapping of the anharmonic observed spectra of Tp(OH) and Tp(OD). As shown for malonaldehyde, the observed spectra can also be reasonably approached in nontunneling anharmonic approximation.[33] More importantly, significant progress has been made on multidimensional quantum mechanical or semiclassical vibration−contortion coupling treatments, as shown by applications to the tunneling malonaldehyde molecule in full 21D.[34−36] A good start has also been made on multidimensional computations for tropolone.[18] The presently computed harmonic spectra obtained for the twelve isoelectronic configurations allow a broad overview and correlation of the vibrational states. The data indicate, for example, that vibrations observed for Tp at 349.1 and 361.1 cm^{-1} should be assigned as $\nu_{14}(a_1)$ and $\nu_{39}(b_2)$ instead of as the reverse,[12,13,15] and that several of the previously considered tautomer-to-SP normal-mode correlations[13,15] in the a_1 symmetry block of Tp should be revised. The latter results are important to the estimation of vibrational state-specific tunneling barriers.

In addition to sketching out features of the effective PES, the normal coordinates are useful as first indicators for the degree of dynamical complexity that can be expected in vibrational state-specific tautomerization processes. This is because in certain vibrational excitations the pairs of identical atoms located across the molecule from one another may be required to exchange unequal vibrational amplitudes as a part of the tautomerization process.[13] This exchange occurs in addition to the transfer of the labile H atom, and to the accompanying exchanges of bond character and associated atom displacements of the equilibrium coordinate values. The redistribution of intramolecular vibrational amplitudes in excited states is, in effect, a tautomerization-induced intramolecular vibrational energy rearrangement (IVR). For complex vibrational states, this dynamical process seems destined to increase the effective multidimensional tunneling path length, that is, to promote quenching of the tunneling process.

The MP2/GEN-computed harmonic fundamental vibrational spectrum of Tp appears in refs 12 and 16, where it was used to assist the analysis of the data observed for Tp(OH) and Tp(OD). The harmonic spectra and PES properties computed for 5Azt, 5AztH$^+$, and Tp bear sufficient similarities that readily resolvable vibrational state-specific tunneling doublets can be expected for all three molecules—not just for Tp.

9. Concluding Discussion

1. 1-H-azepine-4,5-dione, 45Di, has been synthesized,[22] but few of its physical and chemical properties are known. The present MO computations suggest that in the gas phase 45Di has a twisted nonplanar geometry with energy minima at C_2 point group symmetry. The energy at the C_{2v} SP barrier maximum is computed to be only 1.85 kJ mol^{-1} (154 cm^{-1})

above the energy minima, thereby suggesting nonrigid dynamical behavior. The computed bond distances and bond angles roughly approximate standard values, and the nonplanar geometry of 45Di seems attributable to the relative weakness of its π resonance interactions. The computed dipole moment of 9.6 D is probably exaggerated, but its large magnitude implies a solid-state structure commensurate with a high melting point, and a value greater than 280 °C is reported by Bonacorso et al.[22] The predicted nonplanar geometry, nonrigid behavior, high polarity, and plural tentative oligomerization possibilities of 45Di suggest interesting prospective experimental studies on this substance in the gas phase or in solutions. Solvation interactions may, for example, stabilize planar geometry over twisted geometry (section 5). ^{15}N NMR spectroscopy of 45Di dissolved in a carefully characterized CDF_3/CDF_2Cl mixed solvent may be of interest following the work of Shenderovich et al.[37] on hydrogen-bonded complexes formed between collidine and HF or DF in this mixed solvent. The local electric field acting on the F···H···N and F···D···N hydrogen bond linkages was shown to be tunable through the temperature dependence of the dielectric constant of the mixed solvent. Thus, ^{15}N NMR studies in a temperature range near 100 K were interpreted as implying a controllable transfer of the average H-bond linkage between the limiting FH···N and F···HN configurations. Studies of this type on 45Di could reveal details of its N···H···O linkages in linear dimers or oligomers, for example.

2. At the highest MO levels utilized in this work, the energy of gaseous 45Di is estimated to be about 4 kJ mol^{-1} lower than that of its 5Azt isomer. In polar solvents, the relative MO-computed (SCRF) solvation free energies favor 45Di over 5Azt by about 25 kJ mol^{-1}—to agree with the lack of any ^{1}H or ^{13}C NMR evidence for the formation of 5Azt in chloroform solutions of 45Di. However, the MO computations firmly suggest that 5Azt should be a stable substance existing in a well-defined double-minimum PES similar to that of Tp. The C_{2v} PES saddle points and harmonic vibrational spectra computed for Tp and 5Azt are similar in their S_0 electronic states, and their tautomerization properties are expected to match. When 5Azt is synthesized, it may (like Tp with twice the MO-computed dipole moment value) be found to possess a vapor pressure allowing high-resolution spectroscopic studies of the gaseous molecule. The local PES regions for the 5Azt and 45Di isomers are well-separated from one another on the $C_6H_5O_2N$ global PES, and synthetic routes to produce 5Azt from 45Di via protonation−deprotonation reaction routes seem plausible.

3. The MO-computed geometry and other PES properties of $5AztH^+$ resemble those obtained for Tp and 5Azt. This cation seems potentially obtainable through gas-phase or solution-phase protonations of 45Di in reactions that are amenable to spectroscopic monitoring. The MO-computed estimate for the proton affinity at 25 °C and 1 atm is PA(45Di) = 926.8 kJ mol^{-1}. The deprotonation of 45Di in solution by chemical or electrochemical means could produce the $5AzO^-$ anion which, like TpO^-, is of potential interest as a chelator of metal ions.[3,38]

4. It is hoped that this computational research on six stable isoelectronic substances and their C_{2v} SP configurations, 5Azt, $5AztH^+$, $5AzO^-$ as yet unobserved in the laboratory, will encourage new attempts at their experimental syntheses and characterizations. In addition to the broad chemical and biochemical interest of these substances, the 5Azt and $5AztH^+$ molecules are close homologues to tropolone. They are therefore likely to possess internal H-bonding dynamics capable (through the agency of high-resolution spectroscopy) of adding significantly to the understanding of multidimensional tunneling dynamics in excited electronic states as well as in the S_0 ground electronic states.

Acknowledgment. The author is grateful to T. E. Redington for important help and comments on this work. Support of the Welch Foundation during a portion of this research is gratefully acknowledged.

References and Notes

(1) Dewar, M. J. S. *Nature (London)* **1945**, *155*, 50.
(2) Dewar, M. J. S. *Nature (London)* **1950**, *166*, 790.
(3) Pauson, P. L. *Chem. Rev.* **1955**, *55*, 9.
(4) Alves, A. C. P.; Hollas, J. M. *Mol. Phys.* **1972**, *23*, 927.
(5) Alves, A. C. P.; Hollas, J. M. *Mol. Phys.* **1973**, *25*, 1307.
(6) Rossetti, R.; Brus, L. E. *J. Chem. Phys.* **1980**, *73*, 1546.
(7) Tomioka, Y.; Ito, M.; Mikami, N. *J. Phys. Chem.* **1983**, *87*, 4401.
(8) Redington, R. L.; Chen, Y.; Scherer, G. J.; Field, R. W. *J. Chem. Phys.* **1988**, *88*, 627.
(9) Sekiya, H.; Nagashima, Y.; Nishimura, Y. *Bull. Chem. Soc. Jpn.* **1989**, *62*, 3229.
(10) Bracamonte, A. E.; Vaccaro, P. H. *J. Chem. Phys.* **2004**, *120*, 4638.
(11) Redington, R. L.; Redington, T. E. *J. Mol. Spectrosc.* **1979**, *78*, 229.
(12) Redington, R. L.; Redington, T. E.; Montgomery, J. M. *J. Chem. Phys.* **2000**, *113*, 2304.
(13) Redington, R. L.; Sams, R. L. *J. Phys. Chem. A* **2002**, *106*, 7494.
(14) Redington, R. L.; Sams, R. L. *Chem. Phys.* **2002**, *283*, 135.
(15) Redington, R. L.; Redington, T. E.; Blake, T. A.; Sams, R. L.; Johnson, T. J. *J. Chem. Phys.* **2005**, *122*, 224311.
(16) Redington, R. L. *J. Chem. Phys.* **2000**, *113*, 2319.
(17) Wójcik, M. J.; Nakamura, H.; Iwata, S.; Wiktor, T. *J. Chem. Phys.* **2000**, *112*, 6322.
(18) Giese, K.; Kühn, O. *J. Chem. Phys.* **2005**, *123*, 054315.
(19) Knapp, M. J.; Klinman, J. P. *Eur. J. Biochem.* **2002**, *269*, 3113.
(20) Sutcliffe, M. J.; Scrutton, N. S. *Eur. J. Biochem.* **2002**, *269*, 3096.
(21) Antoniou, D.; Caratzoulas, S.; Kalyanaraman, C.; Mincer, J. S.; Schwartz, S. D. *Eur. J. Biochem.* **2002**, *269*, 3103.
(22) Bonacorso, H. G.; Mack, K.-E.; Effenberger, F. *J. Heterocycl. Chem.* **1995**, *32*, 57.
(23) Frisch, M. J.; Trucks, G. W.; Schlegel, H. B.; Scuseria, G. E.; Robb, M. A.; Cheeseman, J. R.; Zakrzewski, V. G.; Montgomery, J. A.; Stratmann, R. E.; Burant, J. C.; Dapprich, S.; Millam, J. M.; Daniels, A. D.; Kudin, K. N.; Strain, M. C.; Farkas, O.; Tomasi, J.; Barone, V.; Cossi, M.; Cammi, R.; Mennucci, B.; Pomelli, C.; Adamo, C.; Clifford, S.; Ochterski, J.; Petersson, G. A.; Ayala, P. Y.; Cui, Q.; Morokuma, K.; Malick, D. K.; Rabuck, A. D.; Raghavachari, K.; Forseman, J. B.; Cioslowski, J.; Ortiz, J. V.; Stefanov, B. B.; Liu, G.; Liashenko, A.; Piskorz, P.; Komaromi, I.; Gomperts, R.; Martin, R. L.; Fox, D. J.; Keith, T.; Al-Laham, M. A.; Peng, C. Y.; Nanayakkara, A.; Gonzalez, C.; Challacombe, M.; Gill, P. M. W.; Johnson, B. G.; Chen, W.; Wong, M. W.; Andres, J. L.; Head-Gordon, M.; Replogle, E. S.; Pople, J. A. *Gaussian 98*, revision A.6; Gaussian, Inc.: Pittsburgh, PA, 1998.
(24) *CRC Handbook of Chemistry and Physics*, 85th ed.; Lide, D. R., Ed.; CRC Press: New York, 2004−2005.
(25) Tanaka, K.; Honjo, H.; Tanaka, T.; Kohguchi, H.; Ohshima, Y.; Endo, Y. *J. Chem. Phys.* **1999**, *110*, 1969.
(26) Shimanouchi, H.; Sasada, Y. *Acta Crystallogr., Sect. B* **1973**, *29*, 81.
(27) Mó, O.; Yáñez, M.; Esseffar, M.; Herreros, M.; Notario, R.; Abboud, J. L.-M. *J. Org. Chem.* **1997**, *62*, 3200.
(28) Bader, R. F. W. *Atoms in Molecules. A Quantum Theory*; Oxford University Press: New York, 1990.
(29) Foresman, J. B.; Frisch, Æ. *Exploring Chemistry with Electronic Structure Methods*, 2nd ed; Gaussian, Inc.: Pittsburgh, PA, 1995−1996; *Gaussian 98, User's Reference*, 2nd ed; Gaussian, Inc.: Pittsburgh, PA, 1994−1999.
(30) Hunter, E. P. L.; Lias, S. G. *J. Phys. Chem. Ref. Data* **1998**, *27*, 413.
(31) Laane, J. *J. Phys. Chem.* **2000**, *104*, 7715.
(32) Bunker, P. R.; Jensen, P. *Molecular Symmetry and Spectroscopy, Second Edition*; NRC Research Press: Ottawa, 1998.
(33) Alparone, A.; Millefiori, S. *Chem. Phys.* **2003**, *290*, 15.
(34) Mil'nikov, G. V.; Nakamura, H. *J. Chem. Phys.* **2001**, *115*, 6881.
(35) Benderskii, V. A.; Vetoshkin, E. V.; Irgibaeva, I. S.; Trommsdorff, H. P. *Chem. Phys.* **2000**, *262*, 393.
(36) Tew, D. P.; Handy, N. C.; Carter, S. *Mol. Phys.* **2004**, *102*, 2217.
(37) Shenderovich, I. G.; Burtsev, A. P.; Denisov, G. S.; Golubev, N. S.; Limbach, H.-H. *Magn. Reson. Chem.* **2001**, *39*, S91.
(38) Diemer, R.; Keppler, B. K.; Dittes, U.; Nuber, B.; Seifried, V.; Opferkuch, W. *Chem. Ber.* **1995**, *128*, 335.